

1 **Relationship of Superoxide Dismutase to Rotator Cuff Degeneration and Tear in a**
2 **Rat Model**

3

4 Hirohisa Uehara, MD^{1,2}, Yoshiaki Itoigawa, MD, PhD¹, Tomoki Wada MD, PhD¹, Daichi

5 Morikawa, MD, PhD¹, Akihisa Koga MD¹, Hidetoshi Nojiri, MD, PhD², Takayuki

6 Kawasaki, MD, PhD², Yuichiro Maruyama, MD, PhD¹, Muneaki Ishijima MD, PhD²

7

8 ¹Department of Orthopaedic Surgery, Juntendo University Urayasu Hospital, Chiba,

9 Japan

10 ²Department of Medicine for Orthopaedics and Motor Organ, Juntendo University

11 Graduate School of Medicine, Tokyo, Japan

12

13 **Corresponding author:** Yoshiaki Itoigawa

14 2-1-1 Tomioka, Urayasu, Chiba, Japan 279-0021

15 Tel: +81-47-353-3111; Fax: +81-47-390-9881; E-mail: yitoiga@juntendo.ac.jp

16

17 **Running Title:** Superoxide dismutase in degenerative RCs

18

19 **Each author's contribution:**

20 Hirohisa Uehara; First author who contributed for all of this study

21 Yoshiaki Itoigawa; Corresponding author who contributed for all of this study

22 Tomoki Wada; Data acquisition and study design

23 Daichi Morikawa; Study design and Interpretation of data

24 Akihisa Koga; Data acquisition

- 25 Hidetoshi Nojiri; Study design and Interpretation of data
- 26 Takayuki Kawasaki; Study design and Interpretation of data
- 27 Yuichiro Maruyama; Study design and Interpretation of data
- 28 Muneaki Ishijima; Study design and Interpretation of data

29 **ABSTRACT**

30 Rotator cuff degeneration is one of the several factors that lead to rotator cuff tears.
31 Oxidative stress and superoxide dismutase have been reported to be related to rotator
32 cuff degeneration; however, the precise mechanism still remains unclear. In this study,
33 we investigated the relationship of oxidative stress and superoxide dismutase to the
34 degeneration of the rotator cuff using rat models. Eighty-four rats were used to create a
35 collagenase-induced rotator cuff injury model (injury model) and a rotator cuff tear
36 model (tear model). The controls were administered saline and had only a deltoid
37 incision, respectively. We evaluated degeneration morphology of the rotator cuff using a
38 degeneration score; dihydroethidium fluorescence intensity, which detects oxidative
39 stress; gene expression; and superoxide dismutase activity. The rotator cuffs in the injury
40 and tear models significantly increased degeneration scores and dihydroethidium
41 fluorescence intensity. On the other hand, gene expression of superoxide dismutase
42 isoform, superoxide dismutase 1, and superoxide dismutase activity were significantly
43 decreased in the injury model but showed no significant difference in the tear model.
44 These findings suggested that superoxide dismutase might not be associated with rotator
45 cuff degeneration after tear but may be involved in degenerative rotator cuff without tear.
46 However, we found that rotator cuff degeneration involves oxidative stress both with and
47 without tear. Based on these findings, it is presumed that different treatments may be
48 appropriate, depending on the state of rotator cuff degeneration, because the mechanisms
49 of the degeneration may be different.

50

51 **Key Terms:** rotator cuff degeneration; rotator cuff tear; oxidative stress; superoxide
52 dismutase; peroxiredoxin

54 INTRODUCTION

55 The factors contributing to rotator cuff tears fall under 2 main categories:
56 extrinsic factors and intrinsic factors. Extrinsic factors include acromion morphology,
57 subacromial spurs, trauma, and shoulder overuse. Intrinsic factors include inflammation,
58 hypovascularity, aging, and degeneration.¹⁻³ Rotator cuff degeneration is one of the
59 characteristics of tears and aging in rotator cuff entheses. Pathologic changes typical of
60 degeneration have been reported to include thinning and disorientation of collagen fibers
61 and loss of cellularity, vascularity, and fibrocartilage mass at the site of cuff insertion.^{3,4}
62 The precise mechanism of rotator cuff degeneration, however, remains unclear.

63 Recently, it was reported that rotator cuff degeneration is caused by oxidative
64 stress,^{3,5,6} an imbalance between oxidation, caused by reactive oxygen species, and
65 reduction, induced by antioxidant systems.⁷ It is still controversial whether oxidative
66 stress can be a primary mechanism of age-related disease. Oxidative damage could lead
67 to the hallmarks contributing to the ageing process, which include genomic instability,
68 attrition of telomere, epigenetic alterations, and loss of proteostasis.⁸ For example, the
69 attrition of telomere, which accelerates aging and increases the risk of age-related
70 diseases, can be caused by oxidative damage because they are highly sensitive to the
71 damage and their repair capacity is less well than other parts of the chromosome.^{9,10}
72 Furthermore, it was reported that oxidative stress is thought to play a pivotal role in the
73 pathological processes implicated in ageing and age-related diseases and the underlying
74 biochemical mechanisms have been clarified in detail.¹¹ For instance, the mitochondrial
75 DNA damages would lead to loss of redox homeostasis, perturbed Ca²⁺ homeostasis,
76 damage to membrane proteins and lipids, as well as to abnormal mitochondrial energy
77 transduction.¹² These modifications are the driving force for further mitochondrial

78 dysfunction and loss of integrity, which will affect cell viability and cellular function.^{12,13}
79 In addition, organs, being high-energy consuming and sensitive to bioenergetic defects,
80 are strongly affected by mitochondrial dysfunctions, resulting in organ-specific
81 pathologies.

82 Superoxide dismutase (SOD) is a major antioxidant enzyme that scavenges
83 reactive oxygen species *in vivo*.¹⁴ There are 3 SOD isoforms, each having a different
84 active center and locality: SOD1 (CuZn-SOD) is localized in the cytoplasm, with Cu/Zn
85 as its active center; SOD2 (Mn-SOD) exists in the mitochondrial matrix, with Mn as its
86 active center; and SOD3 (EC-SOD) is distributed in extracellular fluids, such as synovial
87 fluid, plasma, and lymph, with Cu/Zn as its active center.¹⁴

88 Previous studies showed that SOD1 deficiency induces age-related effects on
89 various tissues.¹⁵ Morikawa et al.^{16,17} found that excessive oxidative stress induced
90 degeneration of rotator cuff enthesis in SOD1-deficient mice. Yoshida et al.¹⁸ reported
91 that SOD activity was not significantly different between rotator cuffs with tears and
92 those without tears although oxidative stress and tendon degeneration in humans were
93 greater in rotator cuffs with tears than in those without. As the reason for no significant
94 difference in SOD activity, Yoshida et al. described that the SOD might be inactivated
95 and not compensable in cases of advanced rotator cuff tears. Chen et al.¹⁹ created an
96 animal rotator cuff injury model in which collagenase injected into the rotator cuff
97 enthesis caused biomechanical weakness and histological degeneration. Hashimoto et
98 al.²⁰ created animal rotator cuff tear models and showed that the rotator cuff was
99 histologically degenerated after the tear. However, the association of rotator cuff
100 degeneration with oxidative stress and SOD in these models has not been investigated.

101 The purpose of this study was to investigate and compare the relationship of
102 oxidative stress and SOD with rotator cuff degeneration in rat injury models with and
103 without tear. We hypothesized that oxidative stress is involved in the degenerative
104 process in rotator cuff injury models with and without tear through different mechanisms
105 of action of SOD.

106

107 **METHODS**

108 **Animals**

109 Eighty-four Sprague–Dawley (SD) rats were used in this study. The rats were maintained
110 and housed with a 12-hour light-dark cycle and allowed free access to food and drinking
111 water. We created two models with injured rotator cuff, the model without rotator cuff
112 tear as “injury model” and the model with rotator cuff tear as “tear model”. This study
113 was approved by the Animal Care Committee of the authors’ institutions.

114

115 **Rotator Cuff Injury Model**

116 All rats were anesthetized with inhalation of sevoflurane. The injury model was
117 produced using a collagenase injection with some modifications to a previous study.¹⁹
118 The acromion was located in the vertex of the right shoulder and 80 U/8μl of type II
119 collagenase (C6885; Sigma-Aldrich, St. Louis, MO, USA) was injected near the
120 supraspinatus tendon under the acromion using a 27-gage needle (NN-2719S; Terumo,
121 Tokyo, Japan). The amount of collagenase was decided as the same amount as in the
122 previous study¹⁹ because we could make rotator cuff injury model without tear and with
123 histological rotator cuff degeneration using the same amount in our preliminary
124 experiments. The injection was performed for 3 consecutive days. On the third day, the

125 skin was incised by 5 mm and the injection was definitely administered (cuff-injury
126 side). The left shoulder served as a control, and was injected with saline (no-injury side).

127

128 **Rotator Cuff Tear Model**

129 Anesthesia was performed in the same manner as in the injury model. The surgery was
130 performed in bilateral shoulders according to previously described methods.²¹ In the
131 right shoulder, the supraspinatus tendon was exposed by splitting the deltoid muscle. The
132 supraspinous tendon was sharply detached from the insertion using a scalpel. The tendon
133 stump was retracted medially by contraction of the rotator cuff muscle so that a U-
134 shaped medium-size tear was created naturally. The overlying deltoid muscle and skin
135 were then closed (cuff-tear side). In the left shoulder, served as a control, the deltoid
136 muscle was split to expose the supraspinatus tendon and the deltoid muscle and skin
137 were immediately closed without rotator cuff resection (no-tear side). All rats were
138 allowed unrestricted activity in the cage.

139

140 **Tissue Preparation**

141 Rats from the injury model and the tear model were euthanized with an overdose of
142 sodium pentobarbital at 3, 7, or 14 days after the injection or surgery. The supraspinatus
143 tendon entheses of the injury models and the stumps of the ruptured supraspinatus
144 tendon of the tear models were harvested and used for analysis. Specimens used for
145 histological studies were cut into 5- μ m frozen sections and stained with hematoxylin-
146 eosin (H&E), alcian blue (AB), or dihydroethidium (DHE) (Life Technologies
147 Corporation, Gaithersburg, MD). We evaluated one section for each staining for each

148 specimen. Other specimens were used for gene expression analysis using quantitative
149 real-time polymerase chain reaction (RT-PCR) and measurement of SOD activity.

150

151 **Histological Evaluation**

152 The H&E stain was used to investigate the morphology of the rotator cuff tissue,
153 including cell form, collagen orientation, vascularity, and cell distribution. Mucin
154 formation was evaluated using AB staining. We used kernechtrot staining as the
155 counterstain for AB staining. Each sample was cut into 5- μ m thick sections and
156 individually stained with H&E or AB. Sections were viewed under a brightfield
157 microscope (for H&E and AB) and/or a polarized light microscope (for H&E). The
158 tissues were evaluated using a scale described as the “degeneration score.” The score had
159 been proposed in a past study,¹⁸ based on previous reports.²²⁻²⁴ The score comprises 7
160 factors: (i) cell morphology, (ii) collagen alignment, (iii) vascularity, (iv) cellularity, (v)
161 ground substance, (vi) fiber structure, and (vii) collagen stainability. Collagen alignment,
162 cellularity, ground substance, fiber structure, and collagen stainability were evaluated
163 one field of view, at 100 \times total magnification. Cell morphology was evaluated four fields
164 of view, at 200 \times total magnification. Vascularity was evaluated ten fields of view, at
165 400 \times total magnification.²⁴ All fields were set at the tendon 200-400 μ m proximal to
166 bone of the enthesis in injury models and no-tear side of tear models or 200 μ m away
167 from the margin of the stump in cuff-tear side of tear models.²⁵ Each factor was
168 evaluated using a 4-point scale. The 7 scores were then combined and the total score for
169 each sample was calculated. All slides were blindly numbered and independently scored
170 by two researchers familiar with musculotendinous histopathology.

171

172 **Measurement of Dihydroethidium Fluorescence Intensity**

173 Dihydroethidium has been mainly used for superoxide detection.²⁶ In this study, DHE
174 staining was performed on the optimum cutting temperature-preserved frozen tissues, as
175 reported in previous studies.^{27,28} Immediately after collection, the frozen samples were
176 cut into 5- μm thick sections and placed on slides for DHE staining. The DHE was
177 adjusted to 10 $\mu\text{mol/l}$ and applied to each tissue section ($\sim 500\text{--}1,000 \mu\text{l}$) so that the
178 entire section was covered. The slides were then incubated in a light-protected,
179 humidified chamber at 37°C for 30 min.

180 After incubation, the slides were washed twice with phosphate-buffered saline and
181 covered with coverslips. All DHE-stained sections were then immediately photographed
182 using a fluorescence microscope (BZ-9000; Keyence Corporation, Osaka, Japan) at
183 settings of 20 \times magnification, 100% fluorescence excitation, and 0.5-s exposure time.
184 The images were randomly numbered for blind evaluation and analysis using ImageJ
185 (NIH, Bethesda, MD) to determine the fluorescence intensity of the DHE-stained cells.
186 The region of interest was set as the standardized field ($100 \times 100 \mu\text{m}^2$) at the tendon
187 200-400 μm proximal to bone of the enthesis in injury models and no-tear side of tear
188 models or 200 μm away from the margin of the stump in cuff-tear side of tear models.
189 Image analysis was performed within the standardized field on a color scale, and the
190 value of the brightest portion in the region of interest was defined as the fluorescence
191 intensity²⁹⁻³¹. DHE fluorescence intensity was calculated based on an average
192 fluorescence intensity of five fields made for each slide.

193

194 **Gene Expression Analysis**

195 In this study, the gene expression of SOD1 SOD2, and peroxiredoxin 5
196 (PRDX5), another antioxidant enzyme,³² were examined. Total RNA from specimens
197 was extracted with RNeasy Mini Kit (Qiagen, West Sussex, UK) according to the
198 protocols provided by the manufacturer. First-strand cDNA was synthesized using a
199 PrimeScript RT Reagent Kit (Takara, Tokyo, Japan). Quantitative real-time polymerase
200 chain reaction (RT-PCR) studies were performed using TB Green Premix Ex Taq
201 (Takara, Tokyo, Japan) and 400 nM of each primer, routinely in duplicate. The primers
202 were designed based on the sequences in the GenBank database (Table 1). The fractional
203 cycle number at which the fluorescence passes the threshold (Ct values) was used for
204 quantification by using a comparative Ct method. Sample values were normalized to the
205 threshold value for β -actin: $\Delta Ct = Ct(\text{experiments}) - Ct(\beta\text{-actin})$. The Ct value of
206 control was used as a reference. $\Delta\Delta Ct = \Delta Ct(\text{experiment}) - \Delta Ct(\text{control})$. The fold
207 change in mRNA expression was calculated by following the formula: $2^{-\Delta\Delta Ct}$.

208

209 **Measurement of SOD Activity**

210 The SOD activity is regulated both by the amount of SOD protein present and the post-
211 translational modifications reducing the activity. Therefore, it is important to confirm the
212 activity, when using SOD.³³ In this study, SOD activity was measured using a process
213 that was based on a previous report.¹⁸ We used an assay kit (Northwest Life Science
214 Specialties, LLC, Vancouver, WA) and measured the total SOD activity at 7 days after
215 the injection or the surgery according to the protocols provided by the manufacturer. The
216 samples were examined soon after collection. These were mixed with beads and
217 phosphate-buffered saline and crushed to prepare 10% tissue homogenates (mg/ μ l). The

218 homogenates were centrifuged (10,000 rpm × 4 min, 4°C) and the supernatant was
219 collected.

220 A microplate assay was performed using a plate reader (Wallac 1420 ARVOsx
221 Multi-label plate reader; Perkin Elmer, Inc., Waltham, MA). 230 µl of assay buffer was
222 added into each well used for testing. 10 µl of the sample or assay buffer (for the blank)
223 was then added, shaken to mix, and left undisturbed for 2 min. Thereafter, 10 µl of
224 hematoxylin reagent was added and immediately mixed with the shaker function of the
225 instrument. The absorbance at 560 nm was recorded every 10 s for at least 5 min.

226 The data were calculated using the following equations. The decomposition rate
227 ($\Delta\text{Abs}_{560\text{ nm/min}}$) was defined from the reaction rate, and the decomposition rates of
228 the sample (Rate_s) and the blank (Rate_b) were then calculated. The percentage for SOD
229 inhibition of the baseline (blank) reaction rate was calculated as follows: %Inhibition =
230 $(1 - \text{Rate}_s / \text{Rate}_b) \times 100$ (%). The SOD activity was found to be approximately 1.25× the
231 measurable percent inhibition of hematoxylin auto oxidation, as established. The final
232 concentration after adjusting the sample dilution was calculated as follows: SOD activity
233 (units SOD/mg protein) = $1.25 \times \% \text{Inhibition} \times (\text{sample dilution factor})$.

234

235 **Statistical Analysis**

236 The Wilcoxon signed-rank test was performed to compare the degeneration score, DHE
237 fluorescence intensity, gene expression, and SOD activity with control sides. Data were
238 presented as mean values ± standard error of the mean. A value of $p < 0.05$ was
239 considered statistically significant. All analyses were performed with GraphPad Prism
240 (version 8; MDF, Tokyo, Japan).

241

242 **RESULTS**

243 **Rotator Cuff Injury Model**

244 *Histological Evaluation*

245 The H&E-stained tissue revealed signs of degeneration in the cuff-injury side (Fig. 1A–
246 D). Collagen alignment was disrupted and broken down in the cuff-injury side under
247 polarized microscopy (Fig. 1E–H). Mucin formation in the ground substance occurred in
248 the cuff-injury side (Fig. 1I–L). The degeneration scores for each item and the total
249 degeneration score were shown in the table (Table 2). The intra-examiner reliability of
250 the degeneration score in the injury model by two examiners was satisfactory: ICC(2,1)
251 = 0.89. Scores of cell morphology at 3 days, collagen alignment at 14 days, vascularity
252 at 3 and 7 days, and fiber structure at 3 days showed a significant increase. The total
253 scores at 3, 7, and 14 days were significantly higher in the cuff-injury side than the no-
254 injury side (Fig. 2A).

255

256 *Measurement of DHE Fluorescence Intensity*

257 Comparison of the histological specimens from injury models showed that the DHE
258 fluorescence intensity was higher in the cuff-injury side than the no-injury side (Fig.
259 1M–P). DHE fluorescence intensity of the cuff-injury side was not significantly different
260 at 3 and 7 days in comparison with the no-injury side but was higher than the no-injury
261 side at 14 days (Fig. 2B).

262

263 *Gene Expression Analysis*

264 In the gene expression profiles in injury models examined by RT-PCR at 3, 7, and 14
265 days after the injection, a decreased expression of SOD1 in the cuff-injury side was

266 observed at 7 days (Fig. 3A). No significant differences were found between the cuff-
267 injury side and the no-injury side regarding either SOD2 or PRDX5 expression (Fig. 3B
268 and C).

269

270 ***Measurement of SOD Activity***

271 The SOD activity (Fig. 3D) was significantly lower in the cuff-injury side (64.4 ± 12.8
272 units/mg protein) than in the no-injury side (123.6 ± 0.3 units/mg protein; $p = 0.002$).

273

274 **Rotator Cuff Tear Model**

275 ***Histological Evaluation***

276 In tear models, H&E and AB stained tissues showed signs of degeneration in the cuff-
277 tear side (Fig. 4A–L). The degeneration scores for each item and the total degeneration
278 score were shown in the table (Table 3). The intra-examiner reliability of the
279 degeneration score in the tear model by two examiners was satisfactory: $ICC(2,1) =$
280 0.91 . Unlike the injury model, scores of cellularity at 7 and 14 days, vascularity at 14
281 days, and fiber structure at 7 and 14 days showed a significant increase. The total scores
282 at 3, 7, and 14 days exhibited significant increases in the cuff-tear side than no-tear side
283 (Fig. 5A).

284

285 ***Measurement of DHE Fluorescence Intensity***

286 Histological specimens from tear models also showed that the DHE fluorescence
287 intensity was higher in the cuff-tear side than the no-tear side (Fig. 4M–P). The DHE
288 fluorescence intensity in the cuff-tear side was increased at 3, 7, and 14 days compared
289 with the no-tear side. (Fig. 5B)

290

291 *Gene Expression Analysis*

292 Gene expression of SOD1 and SOD2 showed no significant difference at all points (Fig.
293 6A and B). On the other hand, a significant decrease of PRDX5 expression in the tear
294 side was recognized at 14 days (Fig. 6E).

295

296 *Measurement of SOD Activity*

297 The SOD activity was 149.6 ± 10.4 units/mg protein in the no-tear side and 183.0 ± 21.2
298 units/mg protein in the cuff-tear side. No significant differences ($p = 0.24$) were found
299 between the two groups (Fig. 6D).

300

301 **DISCUSSION**

302 In this study, we had created the collagenase-induced rotator cuff injury model
303 and the rotator cuff tear model. We demonstrated that the rotator cuffs of both the models
304 showed tissue degeneration and that increased DHE fluorescence intensity detected
305 oxidative stress. There were significant differences in the involvement of SOD between
306 the two models, in that SOD was significantly decreased in the injury model and not
307 significantly different in the tear model.

308 Several previous studies suggested a relationship between oxidative stress and
309 rotator cuff degeneration.^{3,5,6} These studies proposed a signal pathway to suggest that
310 oxidative stress causes rotator cuff degeneration secondary to oxidative stress via matrix
311 metalloproteinase and c-Jun N-terminal protein kinase.^{3,5} These data indicated that
312 increased oxidative stress promoted rotator cuff degeneration through a variety of
313 signals, ultimately leading to the tear. Oxidative stress has been evaluated in many

314 studies with DHE fluorescence intensity, which can mainly quantify superoxide, as one
315 indicator.²⁶ The results of the present study showed that DHE fluorescence intensity was
316 significantly increased in both the injury and the tear models, demonstrating that these
317 models caused an increase of oxidative stress in the rotator cuffs.

318 The antioxidant enzyme SOD activates and decomposes in the presence of
319 reactive oxygen species.¹⁴ In studies using SOD deficient mice, Morikawa et al.^{16,17}
320 found that SOD1 is a crucial gene that inhibits rotator cuff degeneration due to oxidative
321 stress. Fillipin et al.³⁴ showed in rat models that SOD activity in the Achilles tendon after
322 a tear was not significantly different from that with no tear. Yoshida et al.¹⁸ reported that
323 the SOD activity was not significantly different between patients with and without
324 rotator cuff tear; however, degeneration score and DHE fluorescence intensity of the tear
325 group were significantly higher than in the no tear group. The SOD activity is regulated
326 by the amount of all three SOD isoforms, and SOD isoform specificity cannot be
327 examined. Therefore, SOD1 and SOD2 gene expressions which were important for the
328 rotator cuff degeneration¹⁶ and cartilage of the osteoarthritis^{31,35} were investigated using
329 the RT-PCR. Additionally, no studies have examined changes in SOD using animal
330 rotator cuff injury models without tear and tear models. We found that in the injury
331 model, SOD1 expression and SOD activity were significantly decreased at 7 days and
332 DHE fluorescence intensity was significantly increased at 14 days. Scott et al.³⁶ reported
333 that the expression of all three SOD enzymes decreased with increased collagenase gene
334 expression in osteoarthritis cartilage. In the present study, it is possible that SOD1
335 expression was decreased by collagenase administration. It seems that decrease of SOD1
336 may be one of the reasons for the decrease in SOD activity. Collagenase may also have
337 caused post-translational changes in SOD, but it was not investigated and further study

338 should be needed. In any case, the loss of redox balance due to decreased SOD may
339 cause oxidative stress, leading to an increase in DHE fluorescence intensity at 14 days.
340 On the other hand, the tear models showed no significant difference in SOD1,2
341 expression and SOD activity and showed a significant increase in DHE fluorescence
342 intensity at all points. Rotator cuff tissue degeneration and oxidative stress were caused
343 in both models, but the tear model did not involve SOD. Therefore, rotator cuff
344 degeneration without tear and rotator cuff degeneration after tear are supposedly
345 different in the involvement of SOD for the loss of redox balance.

346 Antioxidant enzymes have been reported to include glutathione peroxidase,
347 catalase, and PRDX, in addition to SOD.³⁷ There are 6 PRDX isoforms, all of which
348 participate directly in eliminating hydrogen peroxide (H₂O₂) and neutralizing other
349 oxidizing chemicals.³⁸ Previous studies reported the association between rotator cuff
350 degeneration and PRDX5, which is widely expressed in mammalian tissues and
351 cellularly localized to mitochondria, peroxisomes, and the cytosol. Nho et al.³ reported
352 that cell apoptosis played an important role in the pathway of tendon degeneration from
353 oxidative stress, and Yuan et al.³⁹ noted an overexpression of PRDX5 via transfection in
354 cultured tendon reduced cell apoptosis. Wang et al.⁴⁰ reported that PRDX5 was
355 significantly upregulated in the degenerative rotator cuff compared with the normal
356 rotator cuff, suggesting a compensated response to oxidative stress in the degenerative
357 tendon. On the other hand, a previous study reported that mitochondrial dysfunction
358 contributes to oxidative stress and cell apoptosis during the aging process.⁴¹
359 Furthermore, Takayama et al.⁴² showed that the increase in oxidative stress can also be
360 caused by mitochondrial dysfunction in tendon tissues. In the tear model of our study,
361 SOD was not significantly different; however, DHE fluorescence intensity was

362 significantly increased from 3 days and PRDX5 was significantly decreased at 14 days.

363 It is possible that mitochondrial dysfunction and cell apoptosis may increase oxidative

364 stress in the rotator cuff after tear, and then PRDX5 in mitochondria may be reduced.

365 Previous studies reported that various antioxidants are effective for treating

366 musculoskeletal tissue degeneration. Kim et al.⁴³ showed that oxidative stress induces

367 autophagic cell death in rotator cuff tenofibroblasts, and cyanidin inhibits cell death.

368 Morikawa et al.¹⁶ reported that rotator cuff degeneration in SOD1-deficient mice could

369 be suppressed with vitamin C. Thus, antioxidants could be helpful for the treatment and

370 prevention of rotator cuff tears in patients with oxidative stress. We showed that

371 degenerative rotator cuffs without tear involved SOD1 in the injury model, and

372 degenerative rotator cuffs with tear in the tear model involved a different antioxidant

373 enzyme. It is possible that antioxidants related to SOD may be useful for suppressing

374 rotator cuff degeneration without tear, and that antioxidants related to antioxidant

375 enzymes other than SOD are useful for suppressing rotator cuff degeneration after tear.

376 Which antioxidant might be useful may depend on the state of the rotator cuff

377 degeneration.

378 There were several limitations in this study. First, we investigated the

379 shoulders of SD rats. It is unclear whether the injury model in this study is the same as

380 the degenerative rotator cuffs of humans. A rat rotator cuff injury model was reported by

381 Chen et al.¹⁹ in which rotator cuff degeneration continued until 14 days after collagenase

382 injection and improved at 21 days. We also found rotator cuff degeneration at 3, 7, and

383 14 days in the injury model, with results similar to those in the study. In addition, the

384 control of the injury model was also injected with saline in order to eliminate the effect

385 of the injection based on previous studies.^{19,44} However, the injection of the control

386 potentially causes mechanical trauma. Second, rotator cuff tear models mimic traumatic
387 ruptures. The tear model in our study was different from that in humans, which is caused
388 by the progress of degeneration due to aging. Because our tear model cannot mimic this,
389 we followed the same method as many previous studies that used animal models.
390 Additionally, in the tear model, the time course was limited to two weeks after the tear.
391 The previous studies reported that in the rat rotator cuff tear model, the rotator cuff tears
392 reattached spontaneously unlike in humans.^{45,46} Because the space between the bony
393 insertion site and the tendon stump mostly filled with scar tissue in approximately one
394 week after the tear,^{45,46} we measured in two weeks after the tear. Third, it is still
395 controversial whether DHE is an accurate detector. Although it has been used as a
396 traditional superoxide detector in many studies, some papers have claimed that DHE is
397 oxidized by various molecules, such as H₂O₂, ONOO⁻, and Fenton's reagent and it is not
398 an accurate indicator of superoxide concentration.²⁶ However, the detection of oxidative
399 stress by DHE may be still considered useful. A previous study showed that DHE was
400 especially oxidized by ROS intracellularly,²⁶ and in this study we eliminated the effect of
401 extracellular staining by measuring the brightest intensity of a field, which would be
402 indicated by the intracellular intensity. Therefore, DHE, which can detect intracellular
403 ROS, may be useful. Fourth, we used β -actin as a housekeeping gene for gene
404 expression analysis. It was reported that ROS negatively regulate actin polymerization
405 by driving actin glutathionylation⁴⁷ although other studies have showed that ROS
406 increased actin polymerization^{48,49} and superoxide production induce an increase in
407 filamentous-actin.⁵⁰ β -actin may be affected by ROS, therefore we need further
408 investigation using other housekeeping genes. Fifth, SOD activity was investigated only
409 at 7 days after the injection or the surgery. The previous study¹⁹ reported that the tissue

410 degeneration has been observed from 3 to 14 days. Therefore, we chose at 7 days as an
411 intermediate time point. However, the results of SOD activity at 3 and 14 days, and
412 before 3 days were not evaluated and further investigation is needed.

413

414 **CONCLUSIONS**

415 Tissue degeneration and oxidative stress of the rotator cuff were observed in
416 both the rotator cuff injury and tear models; however, SOD was significantly decreased
417 only in the rotator cuff injury model. These results suggest that SOD might not be
418 associated with rotator cuff degeneration after tear but is involved in the degenerative
419 rotator cuff without tear, although rotator cuff degeneration involves oxidative stress
420 both with and without tear.

421

422

423 **ACKNOWLEDGMENTS**

424 This study was supported (in part) by the grant from the Grant-in-Aid for Scientific
425 Research (C) (18K09081) and the Institute for Environmental & Gender-Specific
426 Medicine, Juntendo University.

427

428 **REFERENCES**

- 429 1. Yamamoto A, Takagishi K, Osawa T, et al. 2010. Prevalence and risk factors of a
430 rotator cuff tear in the general population. *J Shoulder Elbow Surg* 19:116-120.
- 431 2. Maffulli N, Longo UG, Berton A, et al. 2011. Biological Factors in the
432 Pathogenesis of Rotator Cuff Tears. *Sports Med Arthrosc* 19:194–201.
- 433 3. Nho SJ, Yadav H, Shindle MK, et al. 2008. Rotator cuff degeneration: etiology
434 and pathogenesis. *Am J Sports Med* 36:987-993.
- 435 4. Hashimoto T, Nobuhara K, Hamada T. 2003. Pathologic evidence of
436 degeneration as a primary cause of rotator cuff tear. *Clin Orthop Relat Res*:111-
437 120.
- 438 5. Wang F, Murrell GA, Wang MX. 2007. Oxidative stress-induced c-Jun N-
439 terminal kinase (JNK) activation in tendon cells upregulates MMP1 mRNA and
440 protein expression. *J Orthop Res* 25:378-389.
- 441 6. Yuan J, Murrell GAC, Trickett A, et al. 2003. Involvement of cytochrome c
442 release and caspase-3 activation in the oxidative stress-induced apoptosis in
443 human tendon fibroblasts. *Biochimica et Biophysica Acta (BBA) - Molecular*
444 *Cell Research* 1641:35-41.
- 445 7. Finkel T, Holbrook NJ. 2000. Oxidants, oxidative stress and the biology of
446 ageing. *Nature* 408:239–247.
- 447 8. Lopes da Silva S, Vellas B, Elemans S, et al. 2014. Plasma nutrient status of
448 patients with Alzheimer’s disease: systematic review and meta-analysis.
449 *Alzheimers Dement.* 10: 485–502.
- 450 9. von Zglinicki T, 2002. Oxidative stress shortens telomeres. *Trends Biochem. Sci.*
451 27: 339–344.

- 452 10. Blackburn EH, Epel ES, Lin J, 2015. Human telomere biology: a contributory
453 and interactive factor in aging, disease risks, and protection. *Science* 350: 1193–
454 1198.
- 455 11. López-Otín C, Blasco MA, Partridge L, et al, 2013. The hallmarks of aging. *Cell*
456 153: 1194–1217.
- 457 12. Wallace DC, Chalkia D, 2013. Mitochondrial DNA genetics and the
458 heteroplasmy conundrum in evolution and disease. *Cold Spring Harb. Perspect.*
459 *Biol.* 5: a021220.
- 460 13. Lin MT, Beal MF, 2006. Mitochondrial dysfunction and oxidative stress in
461 neurodegenerative diseases. *Nature* 443: 787–795.
- 462 14. Miao L, St Clair DK. 2009. Regulation of superoxide dismutase genes:
463 implications in disease. *Free Radic Biol Med* 47:344-356.
- 464 15. Nojiri H, Saita Y, Morikawa D, et al. 2011. Cytoplasmic superoxide causes bone
465 fragility owing to low-turnover osteoporosis and impaired collagen cross-linking.
466 *J Bone Miner Res* 26:2682-2694.
- 467 16. Morikawa D, Itoigawa Y, Nojiri H, et al. 2014. Contribution of oxidative stress to
468 the degeneration of rotator cuff entheses. *J Shoulder Elbow Surg* 23:628-635.
- 469 17. Morikawa D, Nojiri H, Itoigawa Y, et al. 2018. Antioxidant treatment with
470 vitamin C attenuated rotator cuff degeneration caused by oxidative stress in
471 Sod1-deficient mice. *JSES Open Access* 2:91-96.
- 472 18. Yoshida K, Itoigawa Y, Wada T, et al. 2019. Association of Superoxide - Induced
473 Oxidative Stress With Rotator Cuff Tears in Human Patients. *J Orthop Res*
474 38:212-218.

- 475 19. Chen HS, Su YT, Chan TM, et al. 2015. Human adipose-derived stem cells
476 accelerate the restoration of tensile strength of tendon and alleviate the
477 progression of rotator cuff injury in a rat model. *Cell Transplant* 24:509-520.
- 478 20. Hashimoto E, Ochiai N, Kenmoku T, et al. 2016. Macroscopic and histologic
479 evaluation of a rat model of chronic rotator cuff tear. *J Shoulder Elbow Surg*
480 25:2025-2033.
- 481 21. Thomopoulos S, Hattersley G, Rosen V, et al. 2002. The localized expression of
482 extracellular matrix components in healing tendon insertion sites: an in situ
483 hybridization study. *J Orthop Res* 20:454-63.
- 484 22. Longo UG, Franceschi F, Ruzzini L, et al. 2008. Histopathology of the
485 supraspinatus tendon in rotator cuff tears. *Am J Sports Med* 36:533-538.
- 486 23. Cook JL, Feller JA, Bonar SF, et al. 2004. Abnormal tenocyte morphology is
487 more prevalent than collagen disruption in asymptomatic athletes' patellar
488 tendons. *J Orthop Res* 22:334–338.
- 489 24. Fearon A, Dahlstrom JE, Twin J, et al. 2014. The Bonar score revisited: region of
490 evaluation significantly influences the standardized assessment of tendon
491 degeneration. *J Sci Med Sport* 17:346-350.
- 492 25. Yonemitsu R, Tokunaga T, Shukunami C. 2019. Fibroblast Growth Factor 2
493 Enhances Tendon-to-Bone Healing in a Rat Rotator Cuff Repair of Chronic
494 Tears. *Am J Sports Med.* 47:1701–1712.
- 495 26. Zielonka J, Kalyanaraman B. 2010. Hydroethidine- and MitoSOX-derived red
496 fluorescence is not a reliable indicator of intracellular superoxide formation:
497 another inconvenient truth. *Free Radic Biol Med* 48:983-1001.

- 498 27. Kuroda J, Ago T, Matsushima S, et al. 2010. NADPH oxidase 4 (Nox4) is a
499 major source of oxidative stress in the failing heart. *Proc Natl Acad Sci U S A*
500 107:15565-15570.
- 501 28. Nijmeh J, Moldobaeva A, Wagner EM. 2010. Role of ROS in ischemia-induced
502 lung angiogenesis. *Am J Physiol Lung Cell Mol Physiol* 299:L535-541.
- 503 29. Itoigawa Y, Suzuki O, Sano H, et al. 2015. The role of an octacalcium phosphate
504 in the re-formation of infraspinatus tendon insertion. *J Shoulder Elbow Surg*
505 24:e175-184.
- 506 30. Koike Y, Trudel G, Uthoff H. 2005. Formation of a new enthesis after
507 attachment of the supraspinatus tendon: A quantitative histologic study in rabbits.
508 *J Orthop Res* 23:1433-1440.
- 509 31. Koike M, Nojiri H, Ozawa Y, et al. 2015. Mechanical overloading causes
510 mitochondrial superoxide and SOD2 imbalance in chondrocytes resulting in
511 cartilage degeneration. *Sci Rep* 5:11722.
- 512 32. Schroder E, Ponting CP. 1998. Evidence that peroxiredoxins are novel members
513 of the thioredoxin fold superfamily. *Protein Sci* 7:2465–2468.
- 514 33. Yamakura F, Kawasaki H. 2010. Post - translational mod- ifications of
515 superoxide dismutase. *Biochim Biophys Acta* 1804:318–325.
- 516 34. Fillipin LI, Mauriz JL, Vedovelli K, et al. 2005. Low-level laser therapy (LLLT)
517 prevents oxidative stress and reduces fibrosis in rat traumatized Achilles tendon.
518 *Lasers Surg Med* 37:293-300.
- 519 35. Koike M, Nojiri H, Kanazawa H, et al. 2018. Superoxide dismutase activity is
520 significantly lower in end-stage osteoarthritic cartilage than non-osteoarthritic
521 cartilage. *PLoS ONE* 13:e0203944.

- 522 36. Scott JL, Gabrielides C, Davidson RK, et al. 2010. Superoxide dismutase
523 downregulation in osteoarthritis progression and end-stage disease. *Ann Rheum*
524 *Dis* 69:1502-1510.
- 525 37. Mates JM, Sanchez-Jimenez F. 1999. Antioxidant en- zymes and their
526 implications in pathophysiologic processes. *Front Biosci* 4:D339–345.
- 527 38. Schroder E, Ponting CP. 1998. Evidence that peroxire- doxins are novel members
528 of the thioredoxin fold superfamily. *Protein Sci* 7:2465–2468.
- 529 39. Yuan J, Murrell GA, Trickett A, et al. 2004. Overexpression of antioxidant
530 enzyme peroxiredoxin 5 protects human tendon cells against apoptosis and loss
531 of cellular function during oxidative stress. *Biochim Biophys Acta* 1693:37-45.
- 532 40. Wang MX, Wei A, Yuan J, et al. 2001. Antioxidant enzyme peroxiredoxin 5 is
533 upregulated in degenerative human tendon. *Biochem Biophys Res Commun*
534 284:667-673.
- 535 41. Seo AY, Joseph AM, Dutta D, et al. 2010. New insights into the role of
536 mitochondria in aging: mitochondrial dynamics and more. *J Cell Sci* 123:2533-
537 2542.
- 538 42. Takayama.S, Hirohashi M, Kato M, et al. 1994. Toxicity of quinolone
539 antimicrobial agents. *J Toxicol Environ Health* 45:1-45.
- 540 43. Kim RJ, Hah YS, Sung CM, et al. 2014. Do antioxidants inhibit oxidative-stress-
541 induced autophagy of tenofibroblasts? *J Orthop Res* 32:937-943.
- 542 44. Robertson CM, Chen CT, Shindle MK, et al. 2012. Failed healing of rotator cuff
543 repair correlates with altered collagenase and gelatinase in supraspinatus and
544 subscapularis tendons. *Am J Sports Med* 40:1993-2001.

- 545 45. Barton ER, Gimbel JA, Williams GR, et al. 2005. Rat supraspinatus muscle
546 atrophy after tendon detachment. *J Orthop Res* 23: 259-65.
- 547 46. Gimbel JA, Van Kleunen JP, Mehta S, et al. 2004. Supraspinatus tendon
548 organizational and mechanical properties in a chronic rotator cuff tear animal
549 model. *J Biomech* 37: 739-49.
- 550 47. Sakai J, Li J, Subramanian KK, et al. 2012. Reactive oxygen species-induced
551 actin glutathionylation controls actin dynamics in neutrophils. *Immunity* 37:
552 1037-49.
- 553 48. Taulet N, Delorme-Walker VD, DerMardirossian C. 2012. Reactive oxygen
554 species regulate protrusion efficiency by controlling actin dynamics. *PLoS One*
555 7: e41342.
- 556 49. Moldovan L, Moldovan NI, Sohn RH, et al. 2000. Redox changes of cultured
557 endothelial cells and actin dynamics. *Circ Res* 86: 549–557.
- 558 50. Moldovan L, Irani K, Moldovan NI, et al. 1999. The actin cytoskeleton
559 reorganization induced by rac1 requires the production of superoxide.
560 *Antioxidants & Redox Signaling*. 1: 29–43.
- 561
- 562

563 **TABLES**

564 Table 1. Primers for quantitative real-time polymerase chain reaction (RT-PCR)

Gene	Primers
β -actin	F: 5'-TGACAGGATGCAGAAGGAGA-3' R: 5'-TAGAGCCACCAATCCACACA-3'
SOD1	F: 5'-TGCGTGCTGAAGGGCGACGGTC-3' R: 5'-AATCCCAATCACACCACAAGCCAAGC-3'
SOD2	F: 5'-AATCCCAATCACACCACAAGCCAAGC-3' R: 5'-CCCAGCAGTGGGAATAAGGCCTGTGG-3'
PRDX5	F: 5'-AAAGGAGCAGGTTGGGAGTG-3' R: 5'-GCAGATGGGTCTTGGAACAG-3'

565

566 SOD1, superoxide dismutase isoform 1; SOD2, superoxide dismutase isoform 2;

567 PRDX5, peroxiredoxin 5

568

569

Table 2. The Degeneration Scores of the Injury Model for Each Item and the Total Degeneration Score

	Day3			Day7			Day14		
	control	injury	<i>p</i> value	control	injury	<i>p</i> value	control	injury	<i>p</i> value
Cell morphology	0.5±0.3	2.0±0.0	<0.05	0.5±0.3	1.5±0.5	0.169	0.8±0.5	1.5±0.5	0.343
Collagen alignment	0.5±0.3	2.0±0.4	0.052	0.8±0.3	1.0±0.3	0.052	0.8±0.3	2.0±0.0	<0.05
Cellularity	0.5±0.3	1.0±0.0	0.180	0.5±0.3	1.0±0.0	0.453	0.8±0.3	1.3±0.3	0.257
Vascularity	0.0±0.0	1.3±0.3	<0.05	0.0±0.0	1.5±0.6	<0.05	0.3±0.3	1.3±0.5	0.160
Ground substance	1.0±0.4	1.3±0.3	0.739	0.3±0.3	1.5±0.5	0.069	0.8±0.5	1.3±0.3	0.436
Fiber structure	0.2±0.2	2.5±0.3	<0.05	1.0±0.4	2.5±0.5	0.095	1.0±0.4	2.5±0.5	0.095
Collagen stainability	0.8±0.3	1.5±0.3	0.134	0.8±0.3	1.3±0.3	0.134	0.8±0.3	2.3±0.5	0.063
Total	3.5±0.9	11.5±0.6	<0.05	4.0±1.1	11.8±2.0	<0.05	5.0±1.3	12.0±1.4	<0.05

Table 3. The Degeneration Scores of the Tear Model for Each Item and the Total Degeneration Score

	Day3			Day7			Day14		
	control	injury	<i>p</i> value	control	injury	<i>p</i> value	control	injury	<i>p</i> value
Cell morphology	0.3±0.2	0.7±0.2	0.311	0.2±0.2	1.0±0.4	0.086	0.5±0.2	1.2±0.3	0.137
Collagen alignment	1.2±0.4	1.5±0.3	0.735	1.3±0.5	2.2±0.5	0.240	1.8±0.6	2.0±0.5	0.931
Cellularity	0.7±0.3	1.5±0.3	0.125	0.5±0.2	1.3±0.2	<0.05	0.8±0.3	1.8±0.2	<0.05
Vascularity	0.2±0.2	0.5±0.2	0.282	0.3±0.2	1.3±0.4	0.070	0.0±0.0	0.8±0.3	<0.05
Ground substance	0.8±0.4	1.7±0.4	0.203	0.3±0.3	0.7±0.4	0.461	0.3±0.3	0.8±0.5	0.527
Fiber structure	0.2±0.2	1.3±0.5	0.073	0.3±0.3	1.7±0.4	<0.05	0.2±0.2	1.8±0.3	<0.05
Collagen stainability	0.2±0.2	0.3±0.2	0.595	0.3±0.3	0.3±0.3	0.900	0.3±0.3	0.3±0.3	0.900
Total	3.7±0.4	6.8±0.8	<0.05	2.6±0.7	8.3±1.0	<0.05	3.8±0.9	8.7±1.5	<0.05

573 **FIGURE LEGENDS**

574 Figure 1. Histology of tissue samples from the injury model. A–D, Hematoxylin-eosin
575 (H&E) stain under light microscopy; E–H, H&E stain under polarized microscopy; I–L,
576 alcian blue (AB) stain under light microscopy; M–P, dihydroethidium (DHE) stain under
577 fluorescence microscopy. Bars = 100 μ m.

578

579 Figure 2. Comparison of the injury side and no-injury side of the rotator cuff injury
580 model. A, Degeneration score; B, fluorescence intensity with dihydroethidium (DHE)
581 stain. *; $p < 0.05$.

582

583 Figure 3. Comparison of the injury side and no-injury side of the rotator cuff injury
584 model. A–C, Fold change of SOD1, SOD2, and PRDX5; D, SOD activity. * $p < 0.05$,
585 ** $p < 0.01$. SOD1, superoxide dismutase isoform 1; SOD2, superoxide dismutase
586 isoform 2; PRDX5, peroxiredoxin 5

587

588 Figure 4. Histology of tissue samples from the tear model. A–D, Hematoxylin-eosin
589 (H&E) stain under light microscopy; E–H, H&E stain under polarized microscopy; I–L,
590 alcian blue (AB) stain under light microscopy; M–P, dihydroethidium (DHE) stain under
591 fluorescence microscopy. Bars = 100 μ m.

592

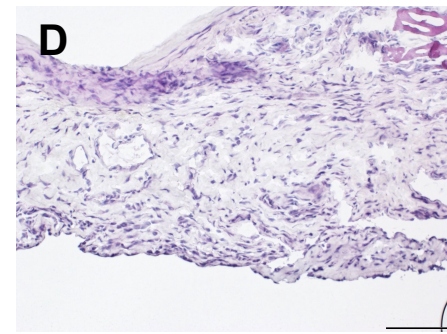
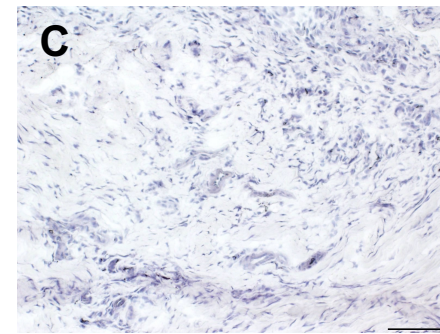
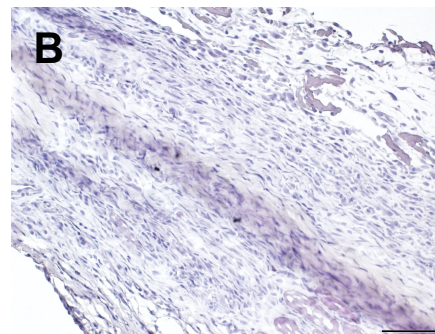
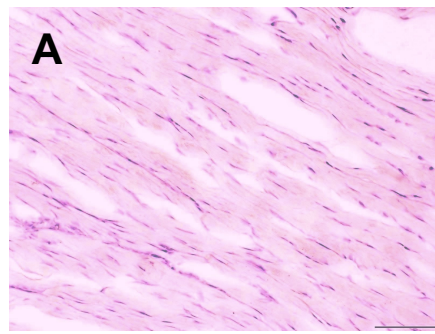
593 Figure 5. Comparison of the tear side and no-tear side of the rotator cuff tear model. A,
594 Degeneration score; B, fluorescence intensity with dihydroethidium (DHE) stain.
595 * $p < 0.05$.

596

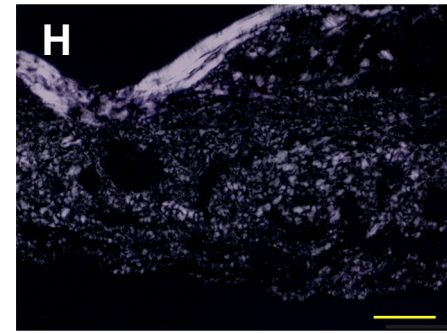
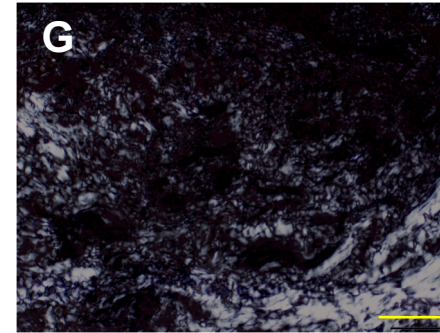
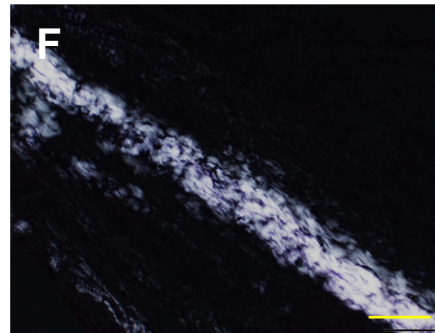
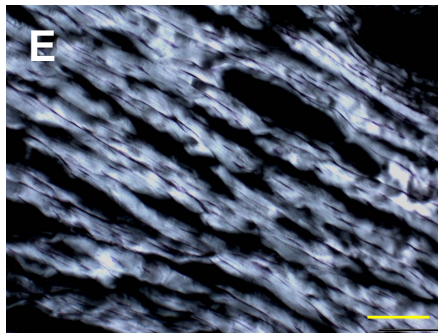
597 Figure 6. Comparison of the tear side and no-tear side of the rotator cuff tear model. A–
598 C, Fold change of SOD1, SOD2, and PRDX5; D, superoxide dismutase (SOD) activity.
599 ★; $p < 0.05$. SOD1, superoxide dismutase isoform 1; SOD2, superoxide dismutase
600 isoform 2; PRDX5, peroxiredoxin 5

Fig.1

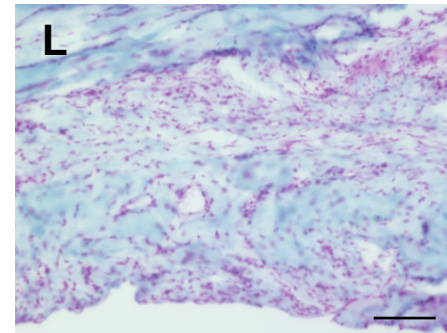
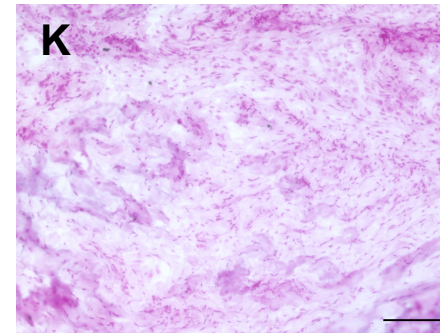
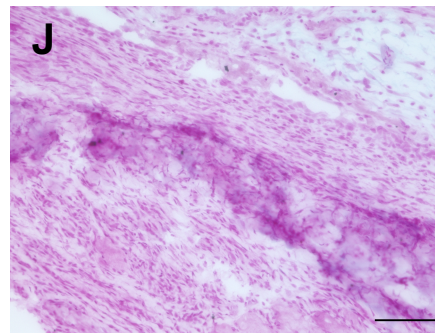
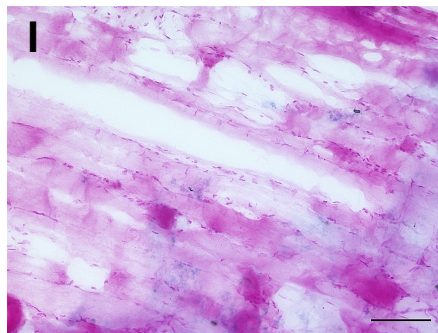
HE staining



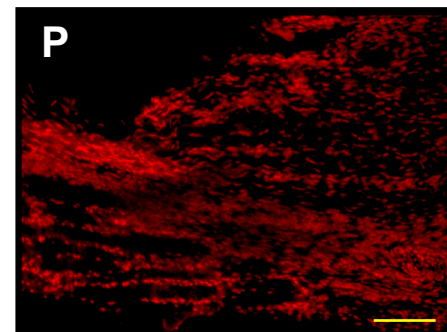
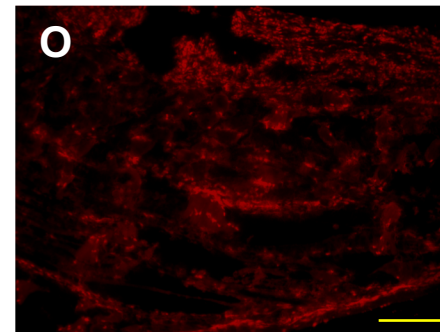
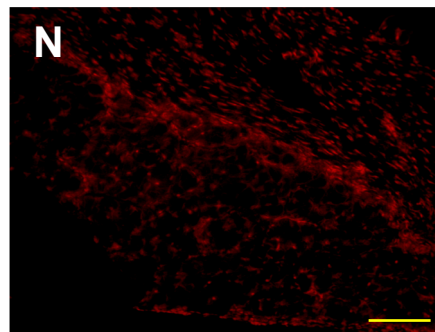
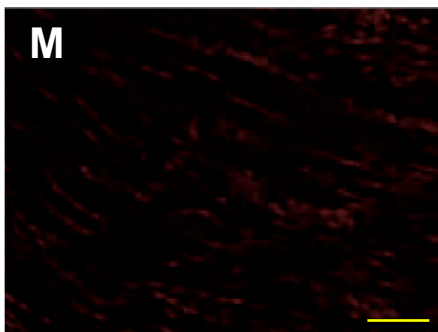
Polarized
microscopy
by HE staining



Alcian blue
staining



DHE staining



no-injury

Day3

Day7

Day14

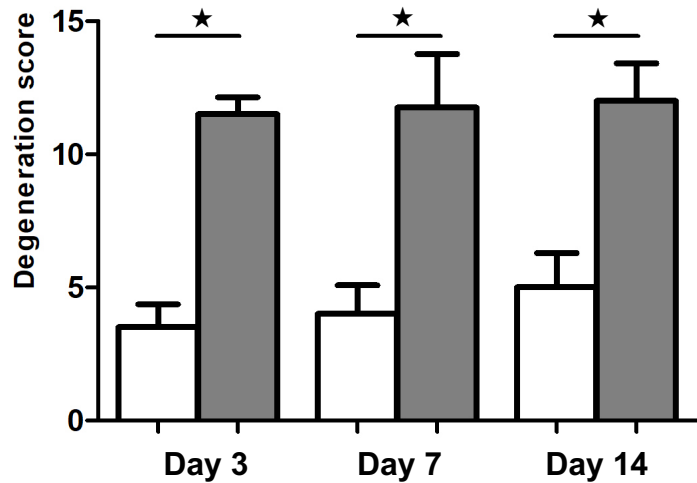
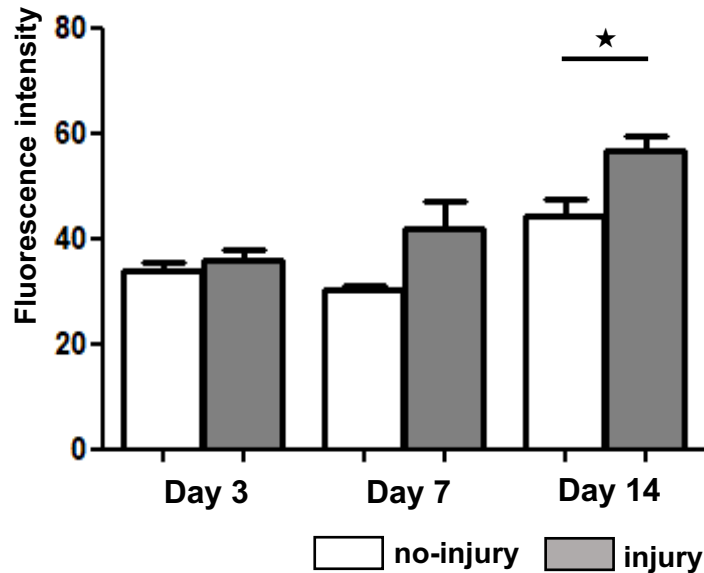
A**Degeneration score****B****DHE intensity**

Fig.2

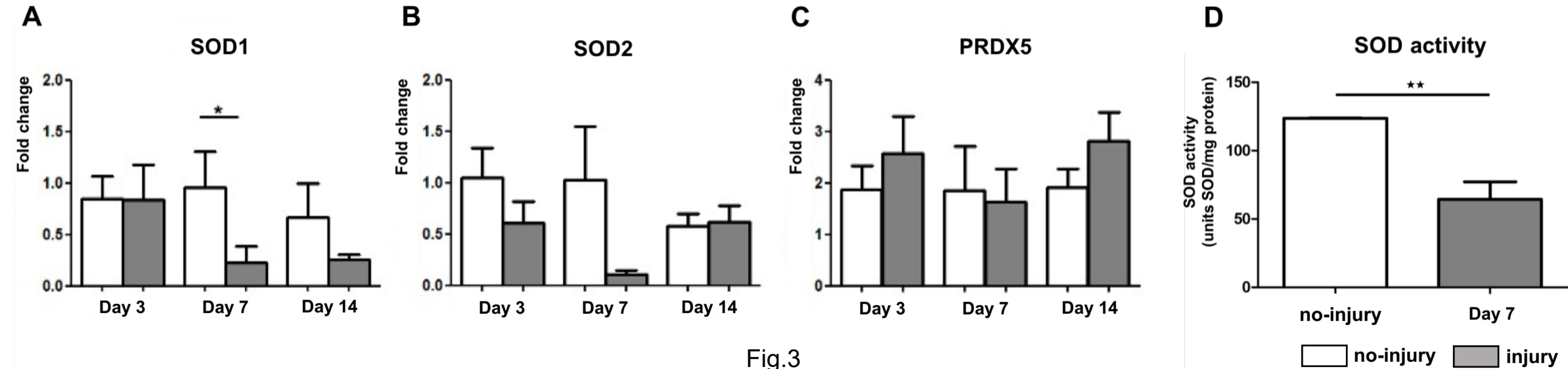
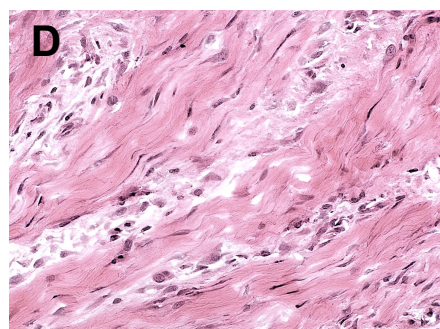
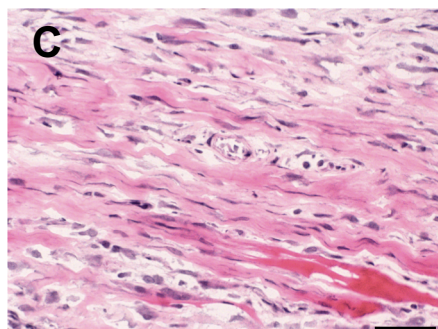
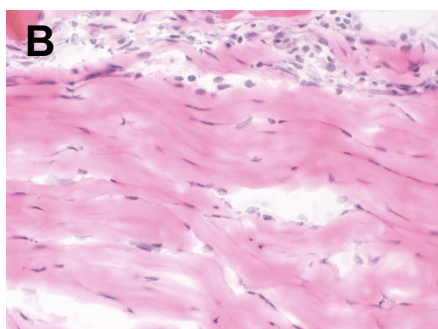
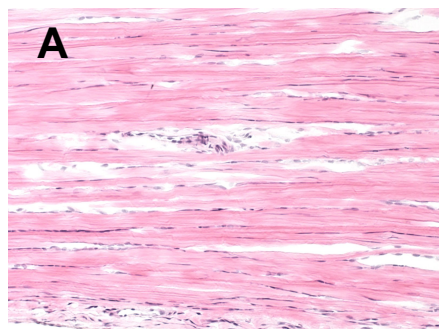


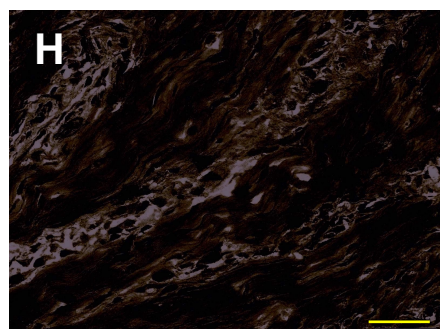
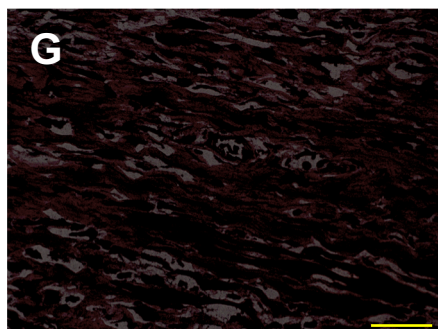
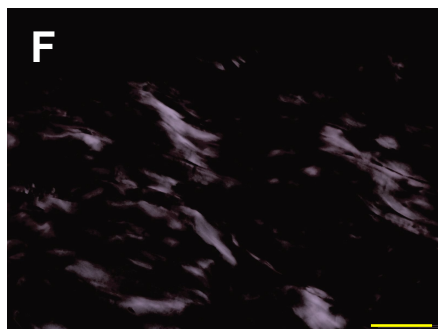
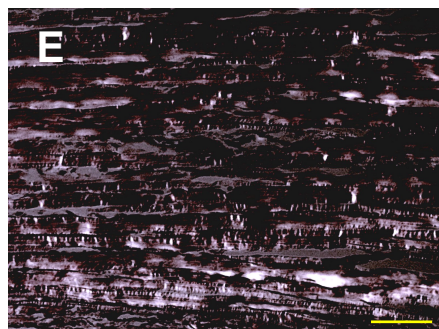
Fig.3

Fig.4

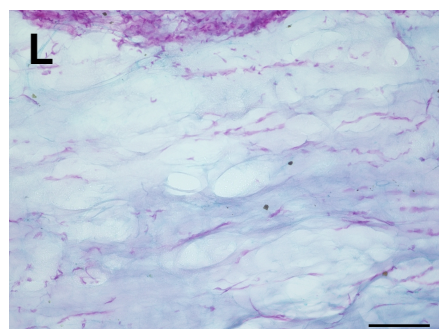
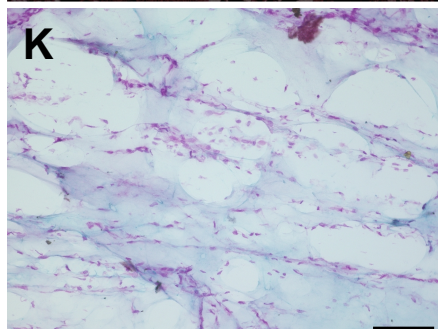
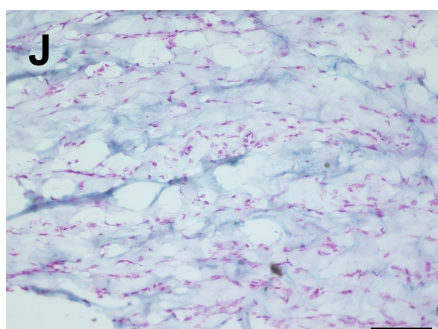
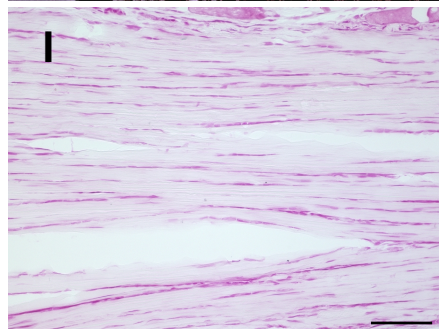
HE staining



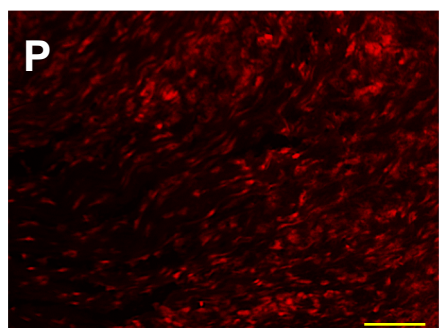
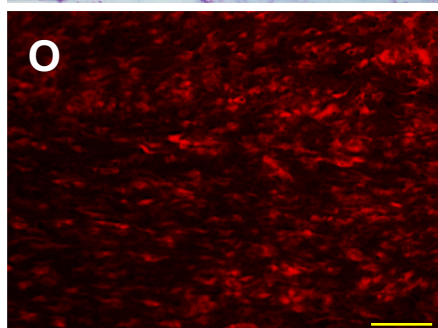
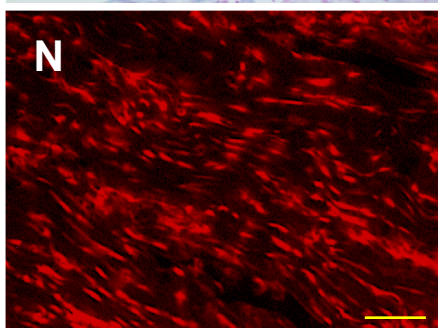
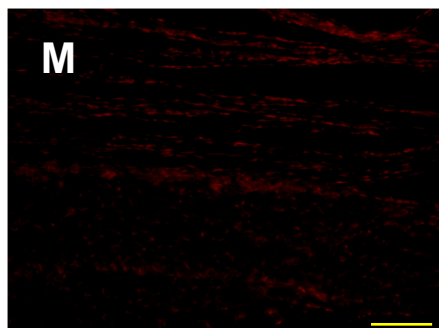
Polarized
microscopy
by HE staining



Alcian blue
staining



DHE staining



no-tear

Day3

Day7

Day14

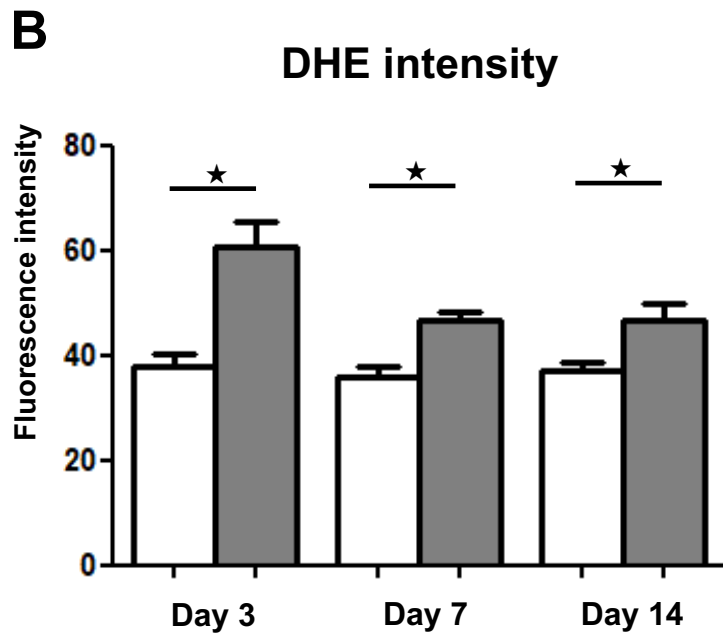
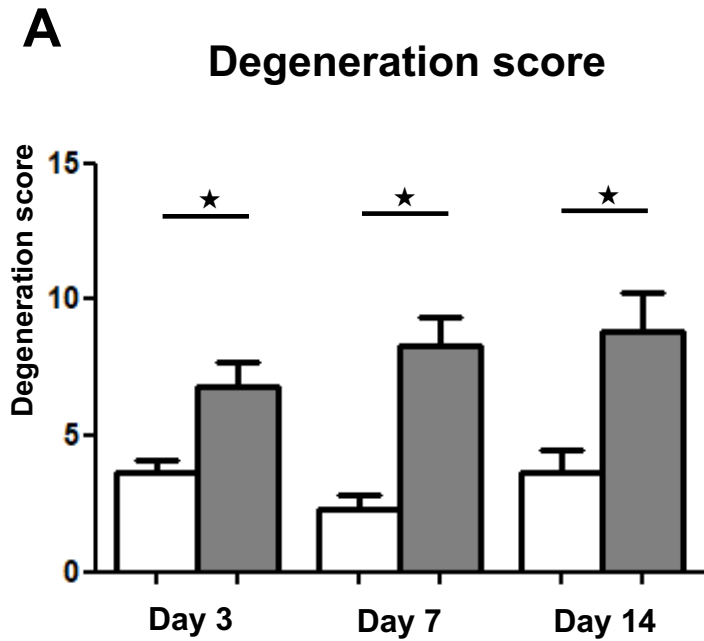


Fig.5

no-tear tear

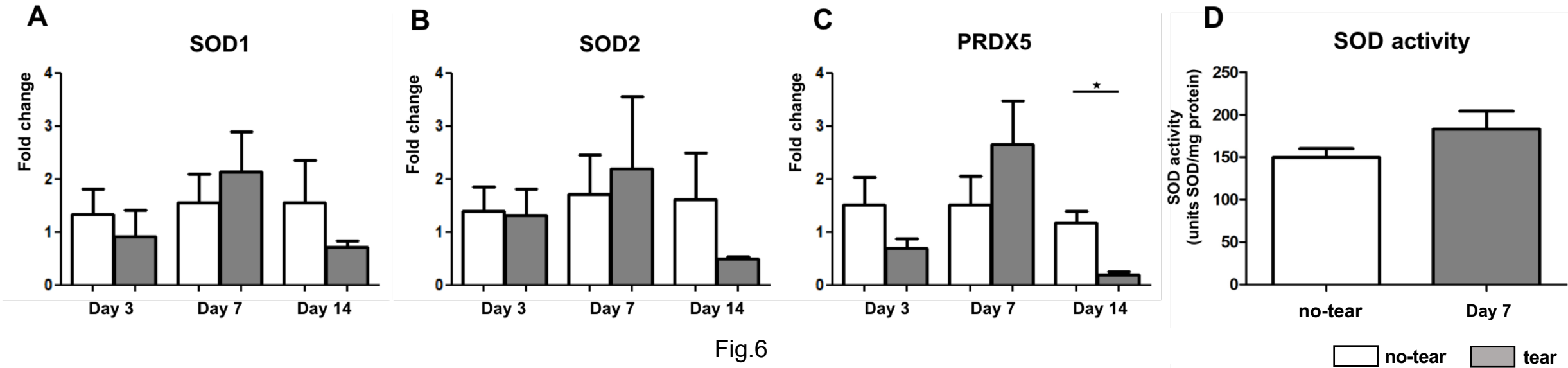


Fig.6